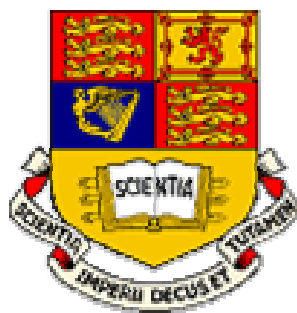


Supramolecular Chemistry of Nanomaterials

Joachim Steinke

Ramon Vilar

Lecture 8 – Templating of Complex Systems



Department of Chemistry
**Imperial College of Science,
Technology and Medicine**

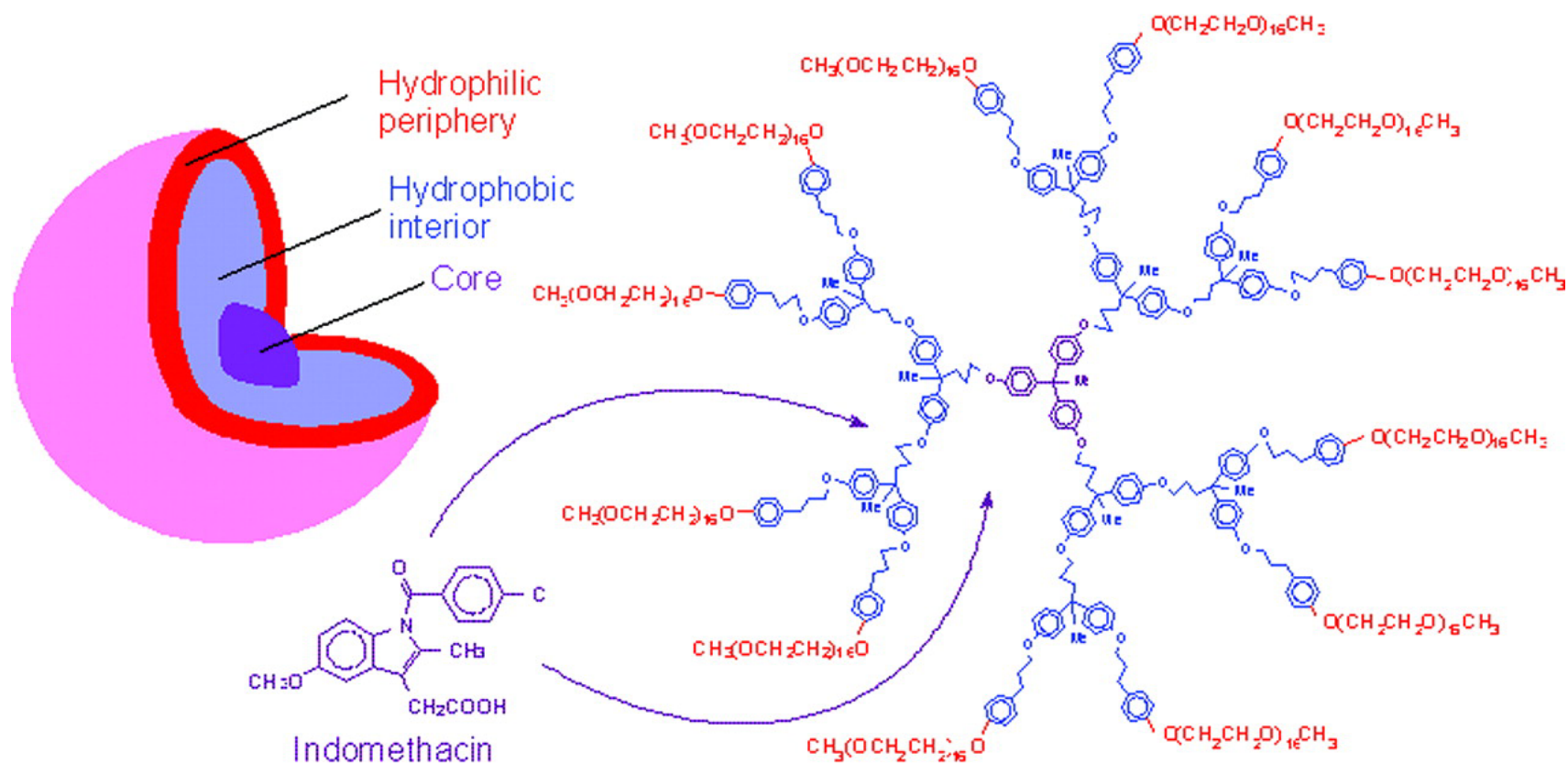
r.vilar@ic.ac.uk

j.steinke@ic.ac.uk

Lecture Content

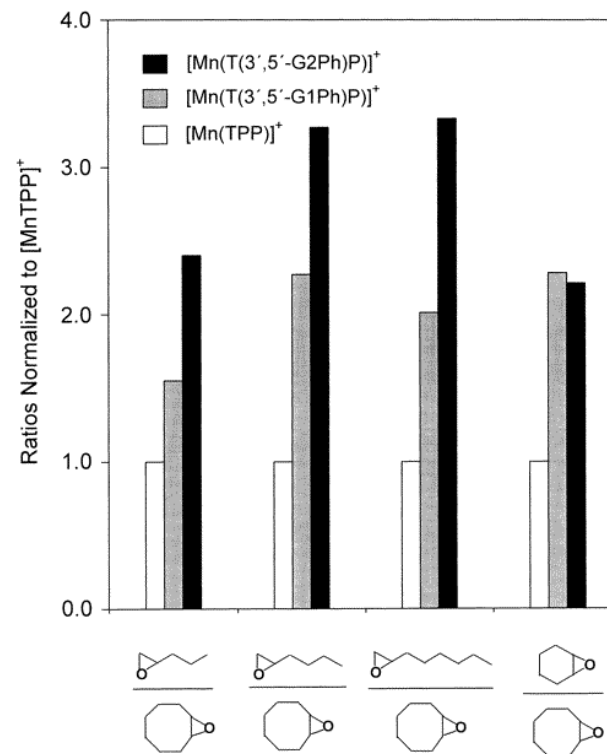
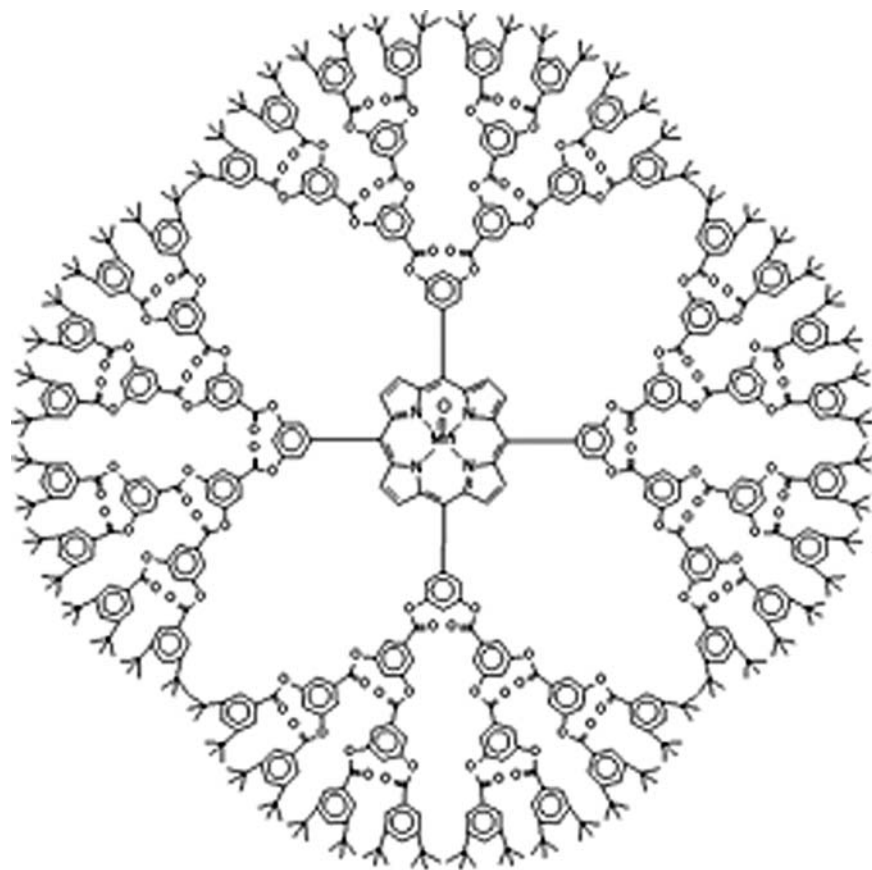
- Dendrimers – Potential applications
- Supramolecular polymers (non-covalent)
- 1-D Templating
- 2-D Templating
- 3-D Templating

Dendrimer – Unimolecular Micelle



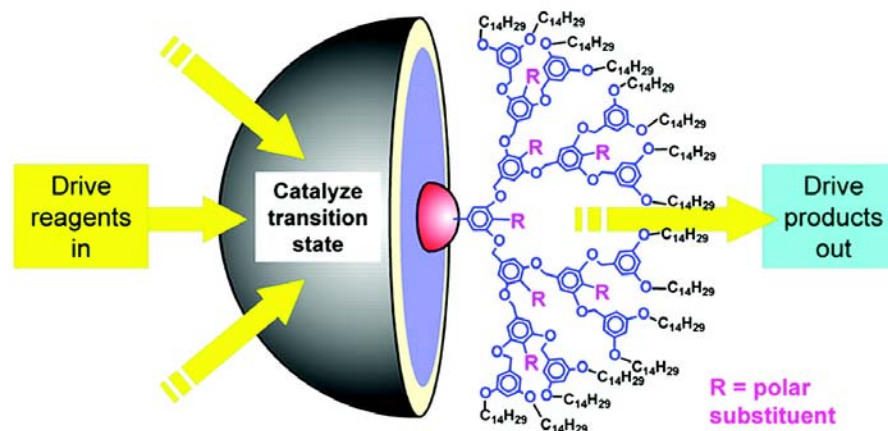
Dendritic "unimolecular micelle" used for the slow release of indomethacin.

Dendrimers - Catalysts

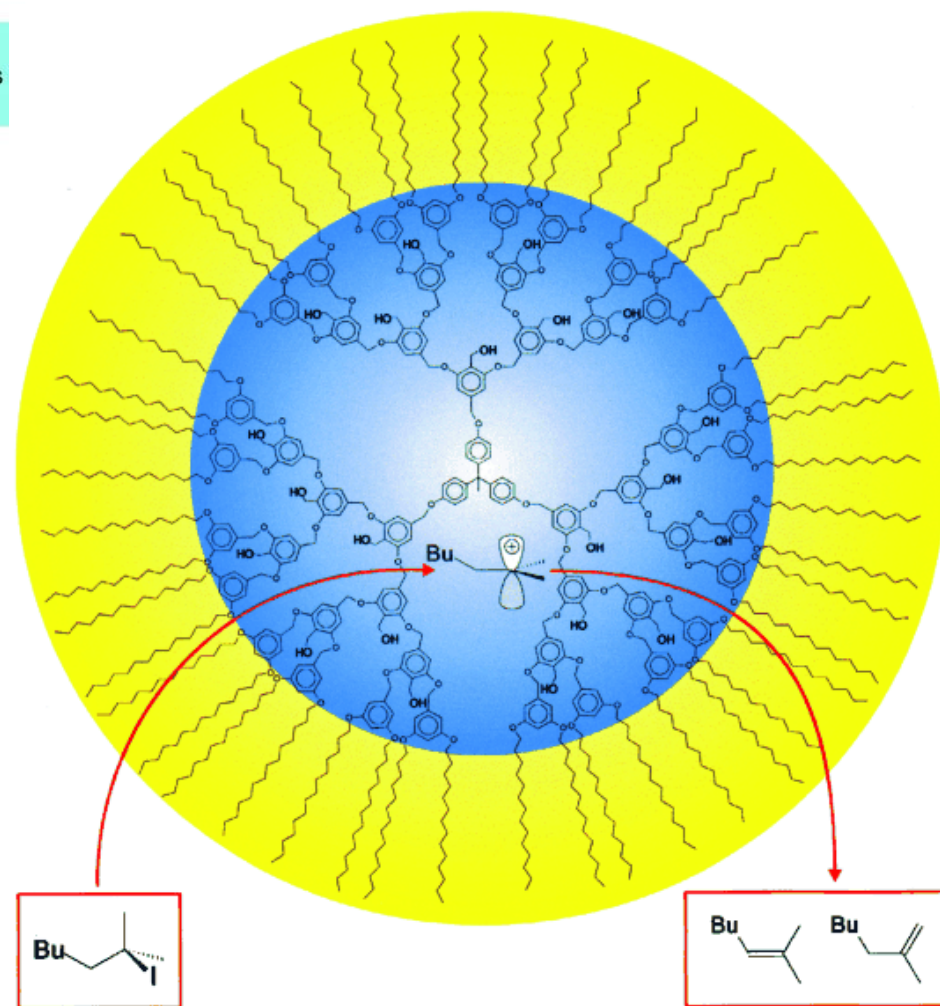


Epoxidation results for the intermolecular mixture of alkenes. The ratios of the epoxides are normalized with respect to corresponding $[\text{Mn}(\text{TPP})]^+$ values.

Dendrimer - Nanoreactor



A dendritic nanoreactor providing both catalysis and rapid mass transfer.



Dendrimer – Light Harvesting

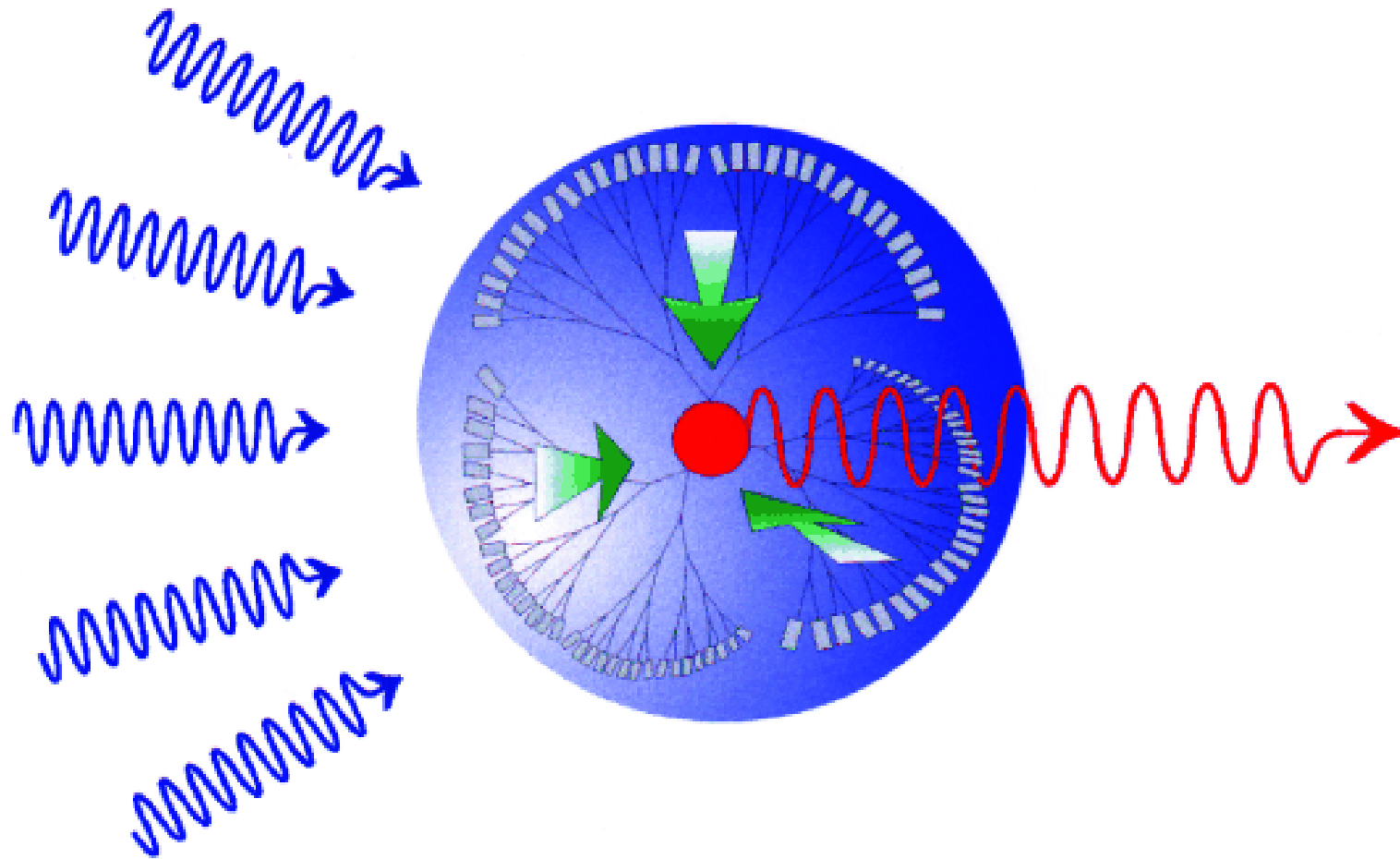
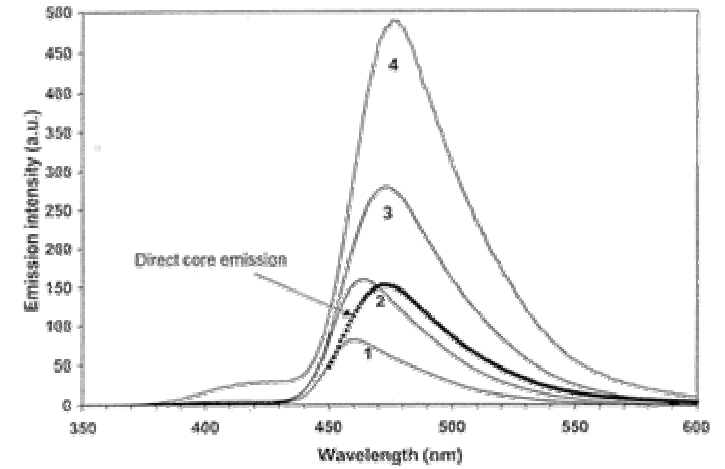
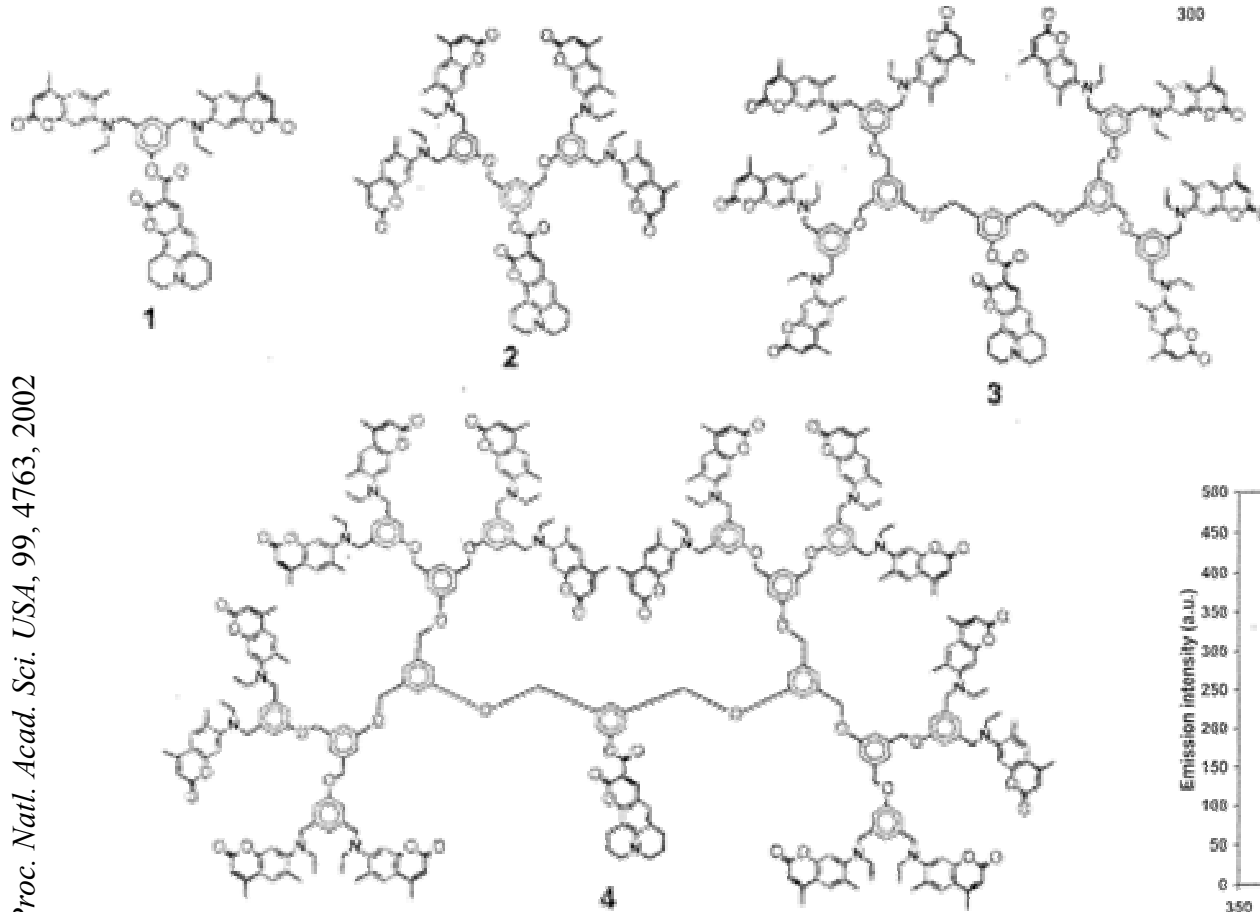
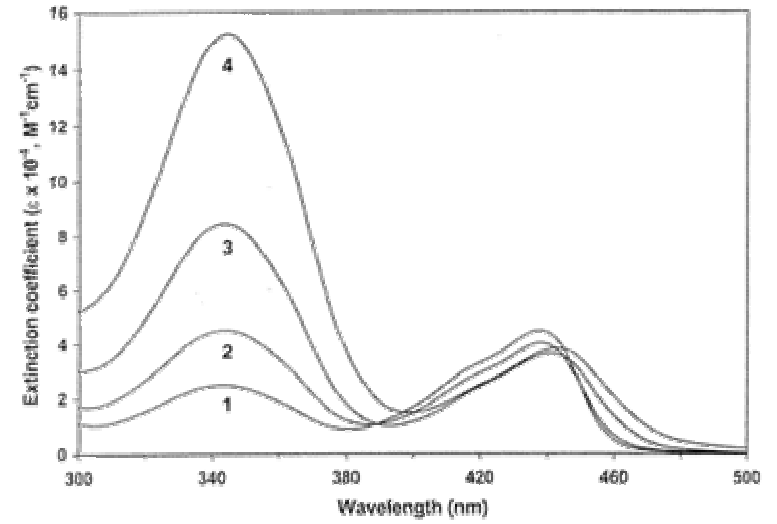


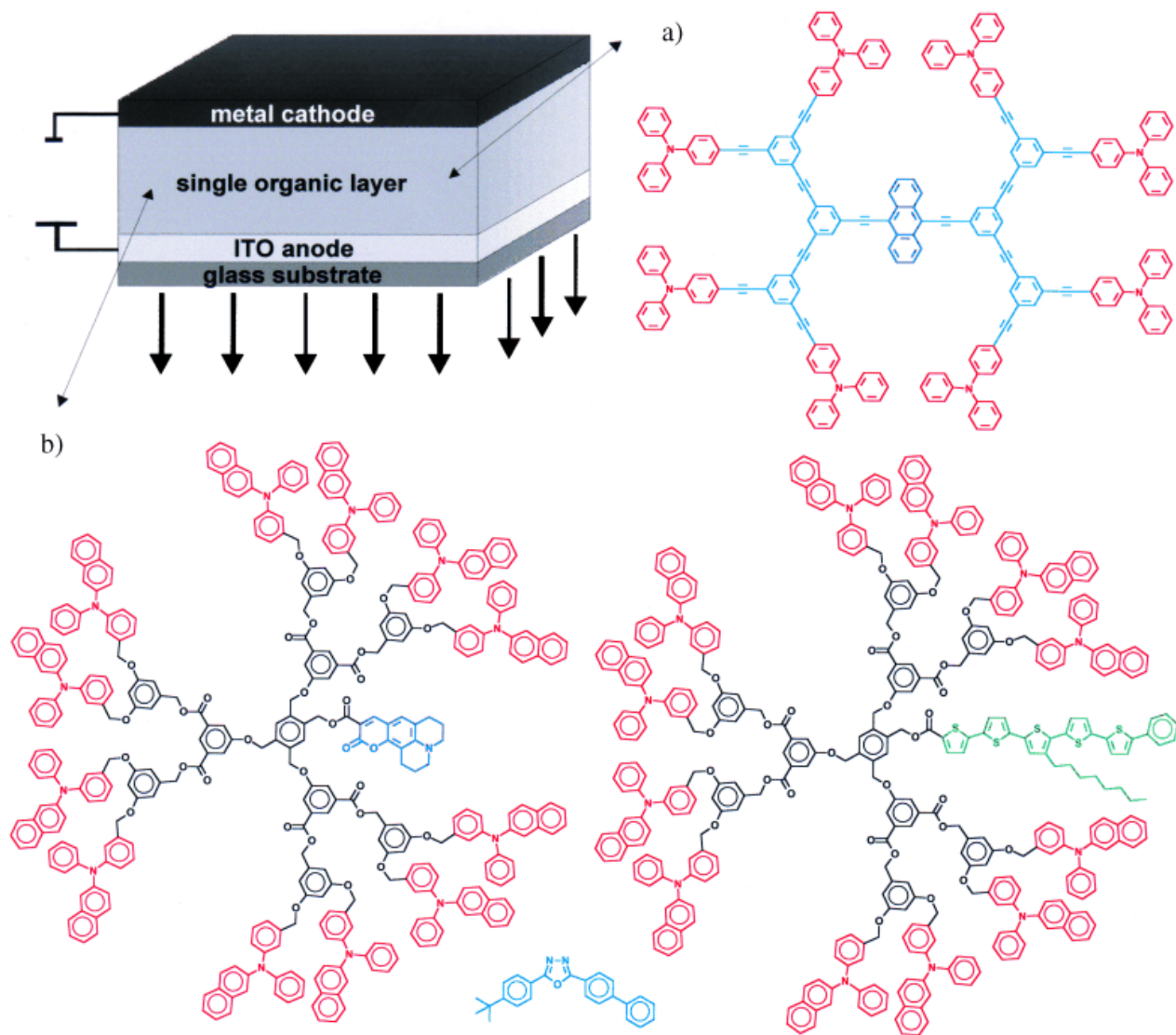
Illustration of a dendritic light-harvesting antenna. The absorption of light of a broad spectral range by peripheral chromophores leads to an enhanced emission from the core (red) as a result of efficient energy transfer (green arrows).

Dendrimer – Light Harvesting

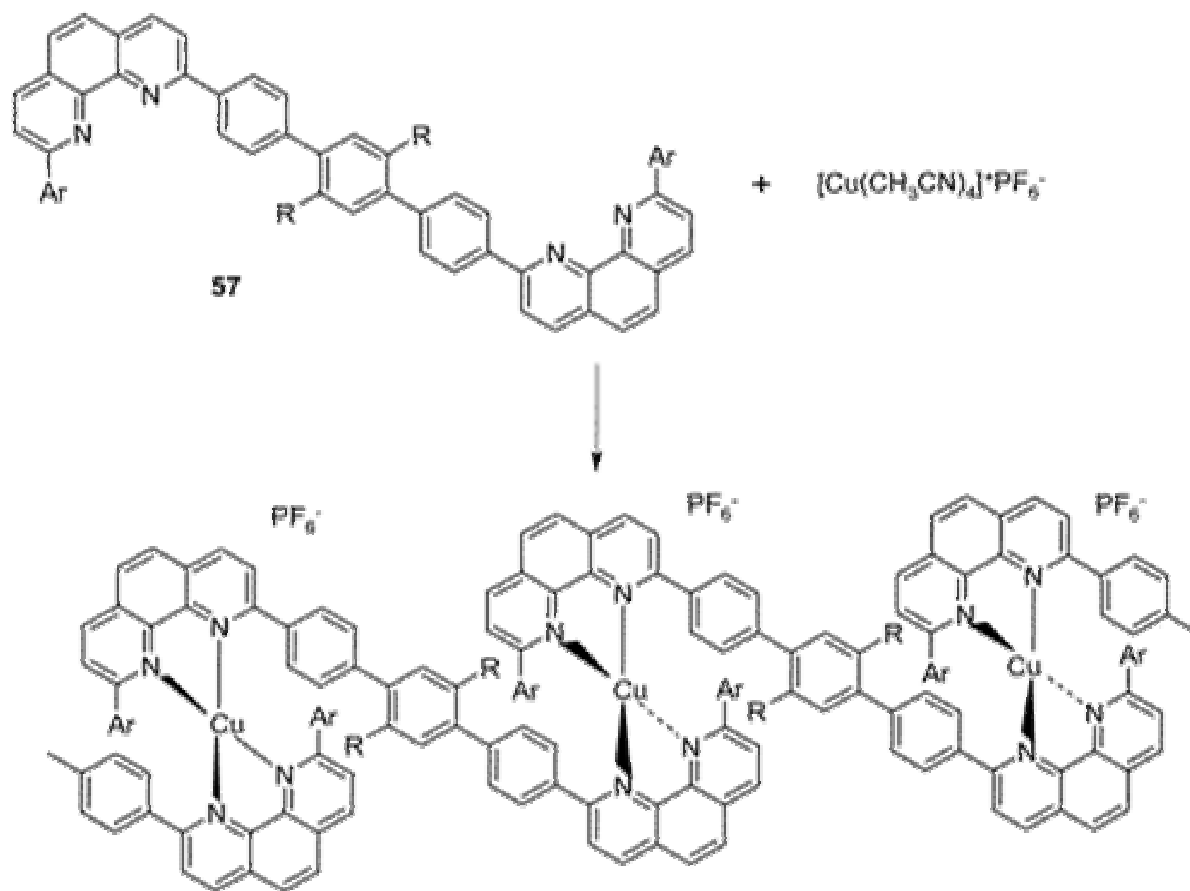


Dendrimers - OLEDs

Single layer organic light-emitting diodes consisting of one component (a) or multiple components (b) for color tunability. Hole-transporting units are shown in red, electron-transporting units in cyan, and the lumophores in their respective emission color.

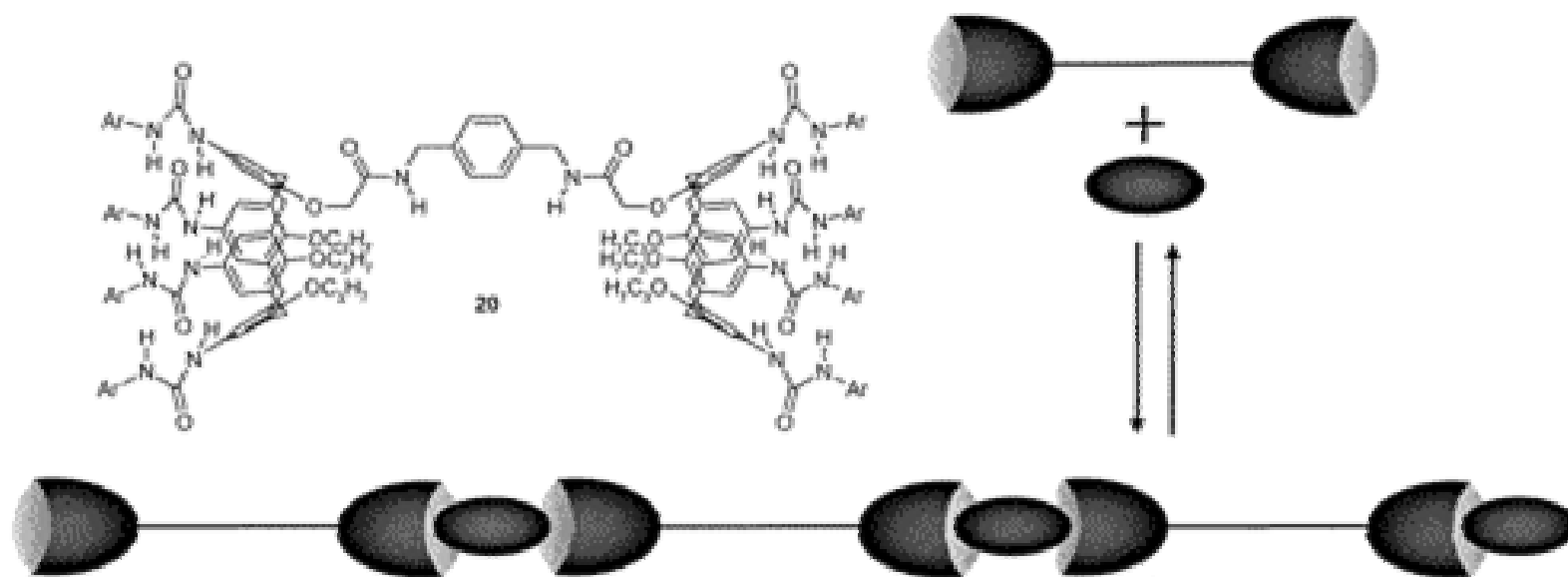


Supramolecular Polymers



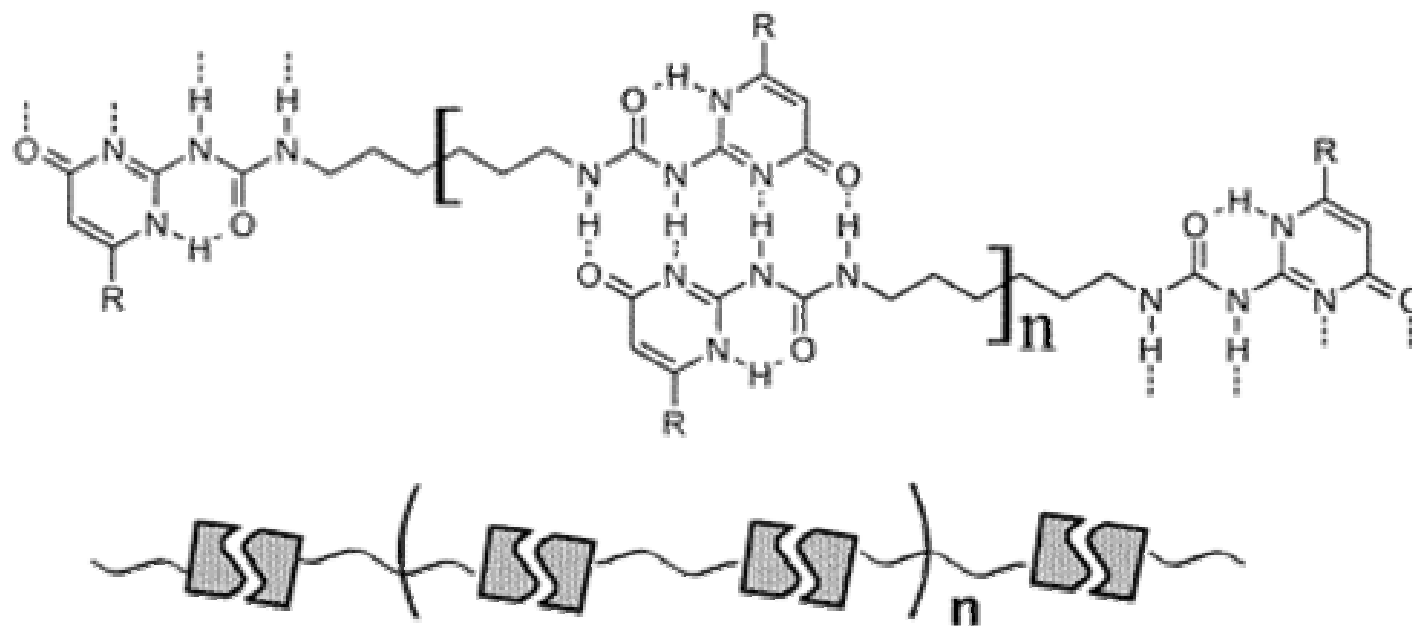
Bifunctional metal complexing **57** and its mode of polymerization upon addition of Cu^+ .

Supramolecular Polymers

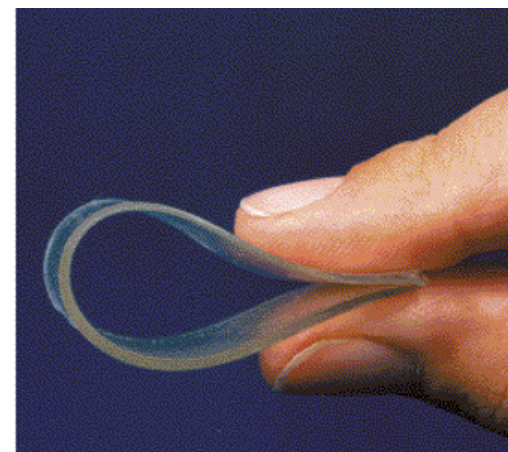
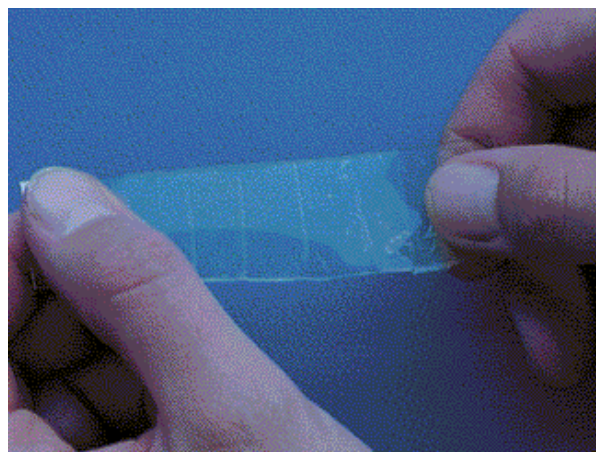


Bifunctional calixarene derivative **20** and a cartoon-like representation of its polymerization induced by small molecules.

Supramolecular Polymers



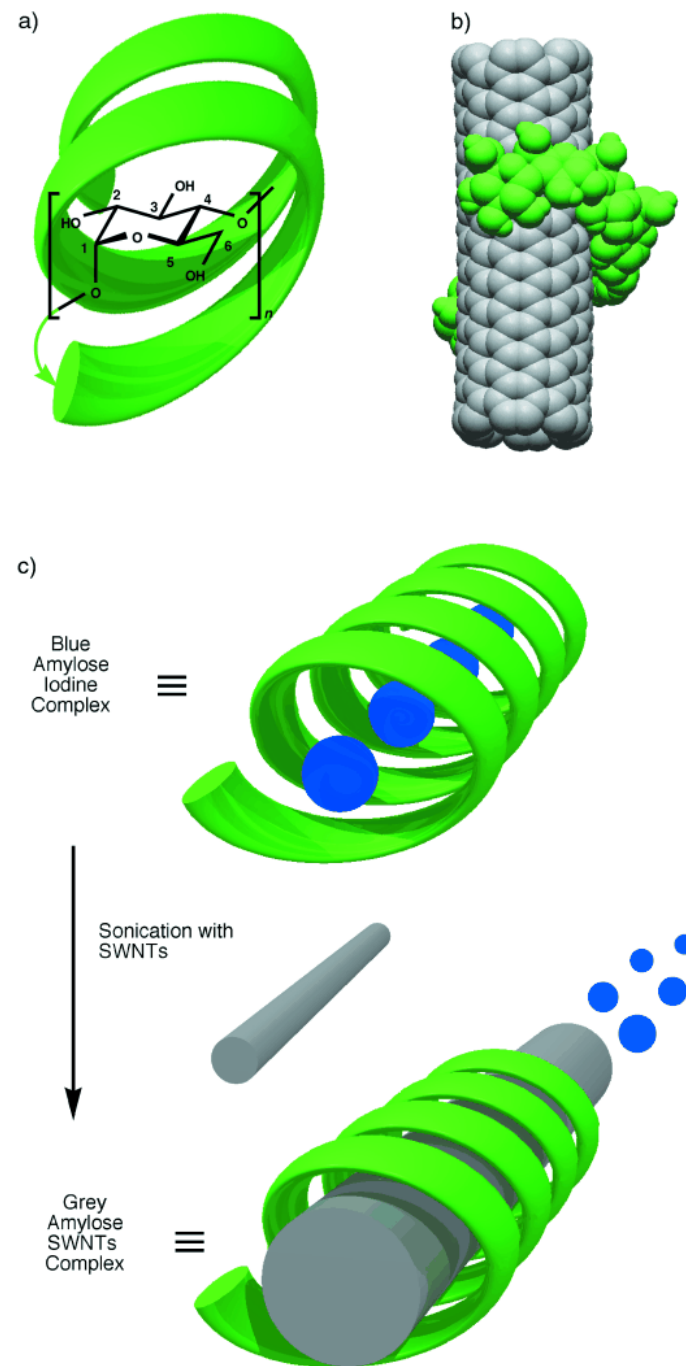
Polymeric assembly of a bifunctional ureido-pyrimidinone derivative.



Templating – 1-D

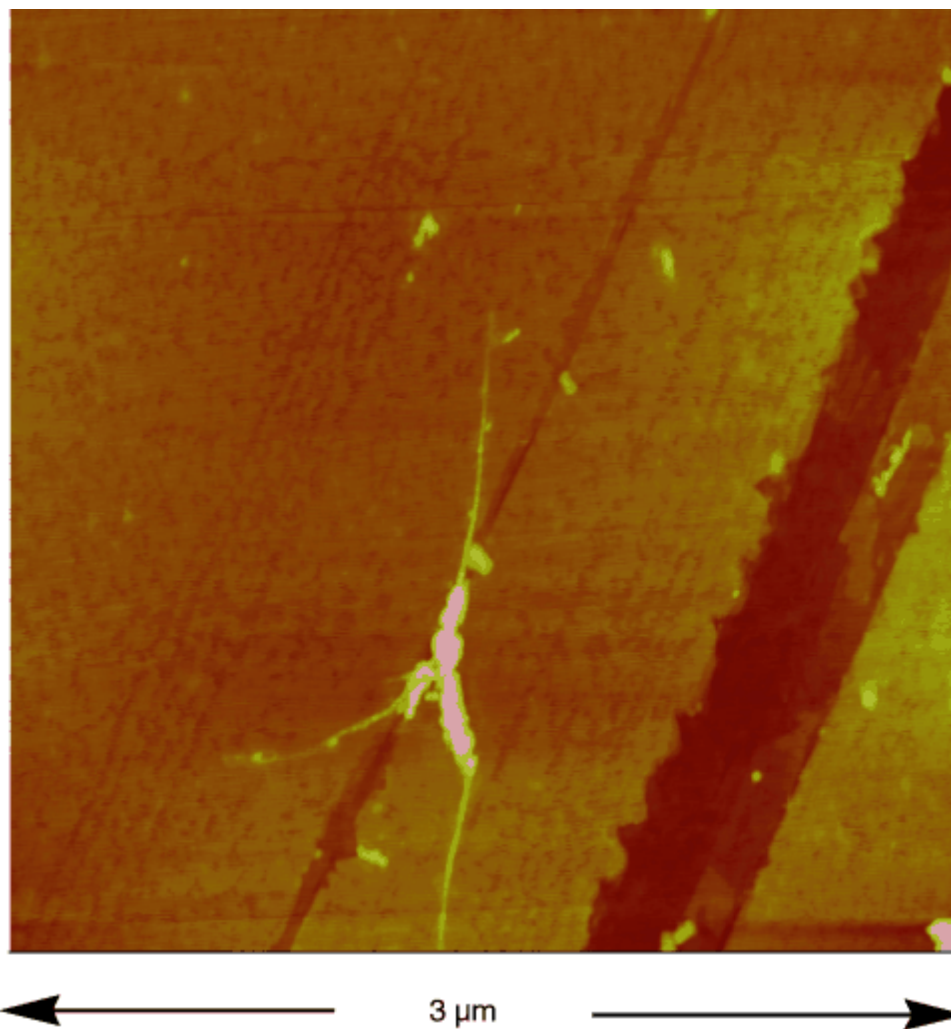
Starched Nanotubes

a) Schematic representation of the left-handed helix adopted by amylose when it complexes with small molecules. One α -1,4-linked D-glucopyranose residue, with its numbering system is overlaid on the helix. b) Space-filling representation of the result of computer modeling (molecular mechanics and molecular dynamics simulations using the solvation model for water) between a short (6,6)-SWNT and maltooctaose. c) Schematic representation of the pea-shooting type of mechanism whereby carbon nanotubes displace iodine molecules from the amylose helix.



Templating – 1-D

An AFM image of isolated bundles of starch-wrapped SWNTs on a mica surface. Amorphous polysaccharide material is seen to aggregate with the nanotubes mostly at junctions between bundles.

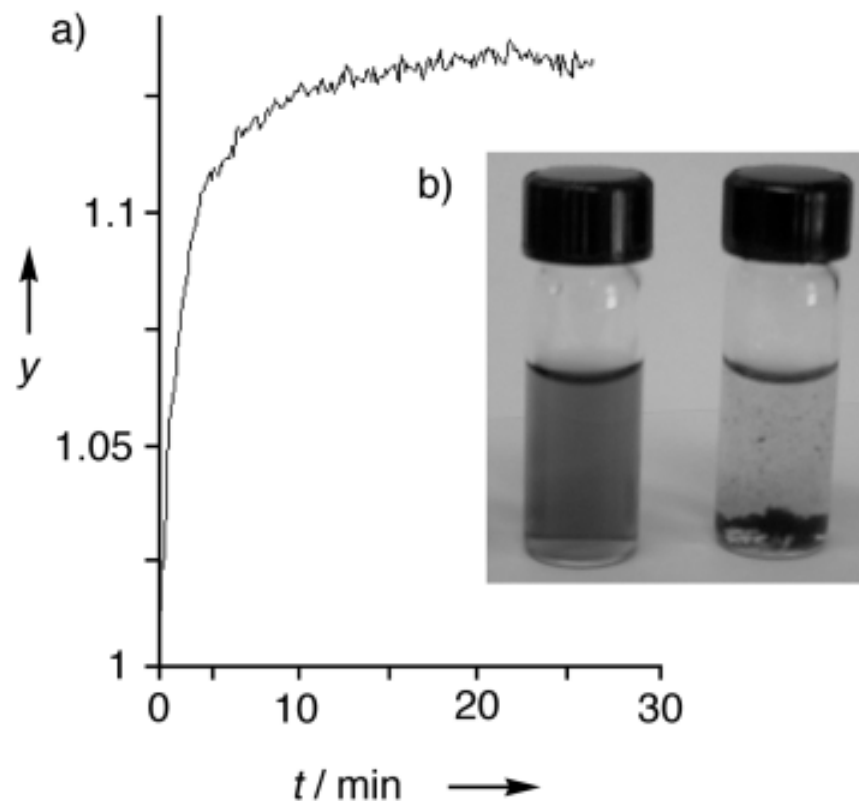


Templating – 1-D

Enzymatic hydrolysis of the starch-SWNT complex.

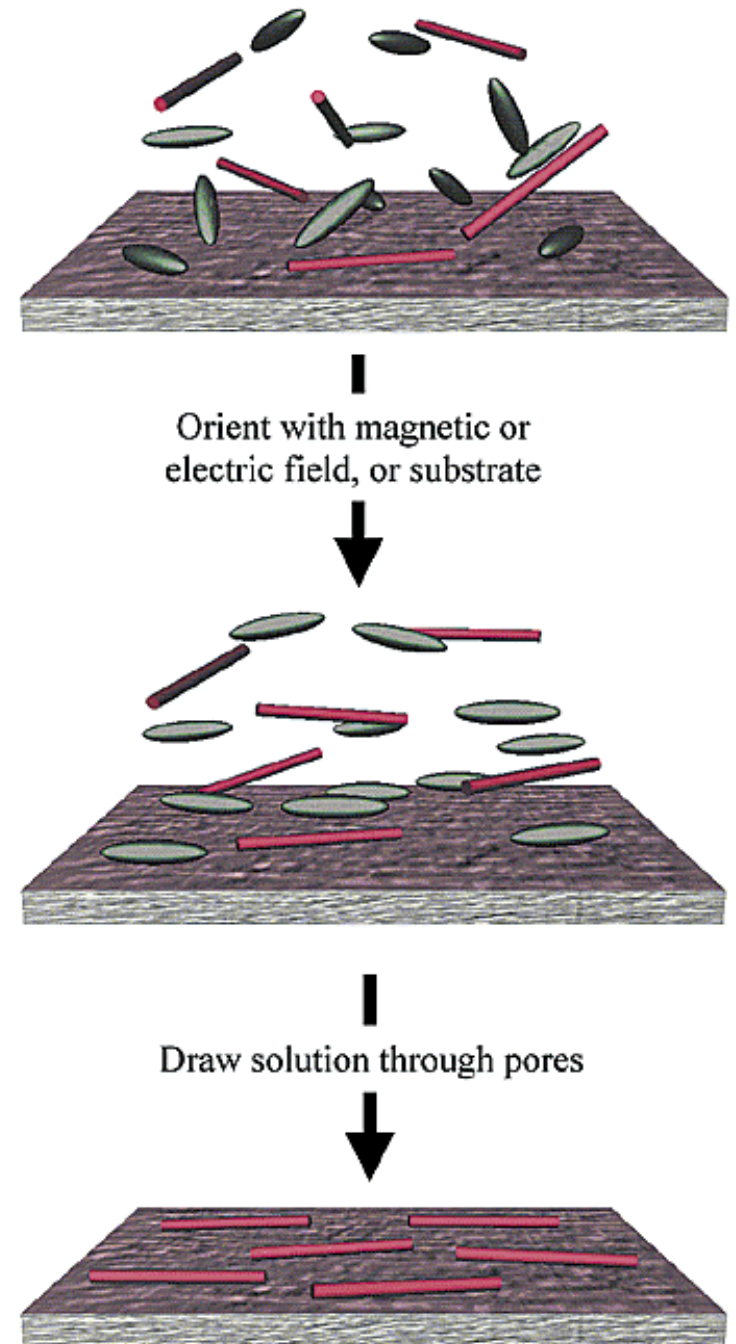
a) changes (y is the refraction in arbitrary units) in light scattering upon addition of amyloglucosidase and

b) a photograph of vials containing the complex before (left) and after (right) addition of the enzyme.



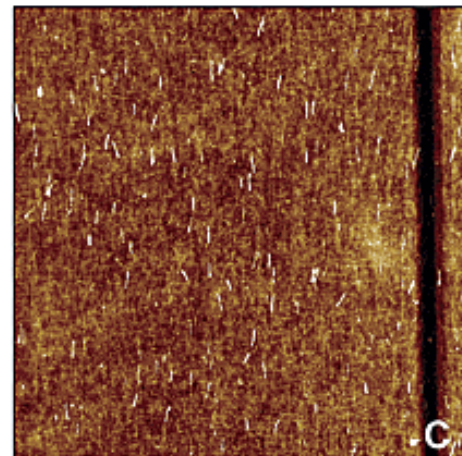
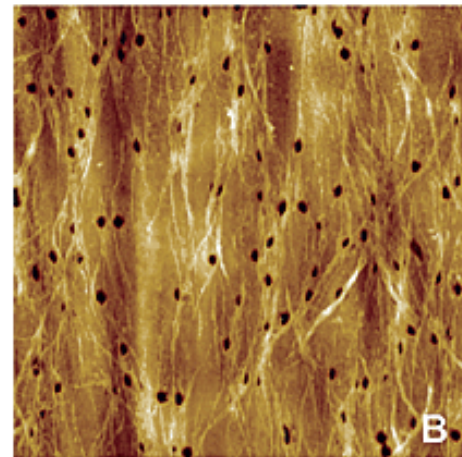
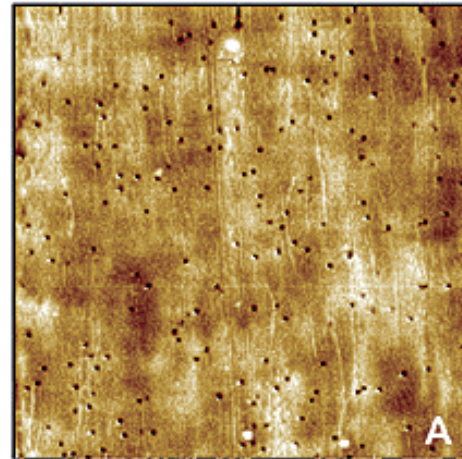
Nanotubes - Organisation

Organizing CNTs with LC solvents. (a) A droplet of liquid crystal (ellipsoids) with suspended carbon nanotubes (rods) is applied to a porous membrane substrate. (b) The bulk LC is then aligned using a grooved surface or external field, which in turn orders the nanotubes. (c) The LC is drained through the porous membrane leaving behind an ordered nanotube film.



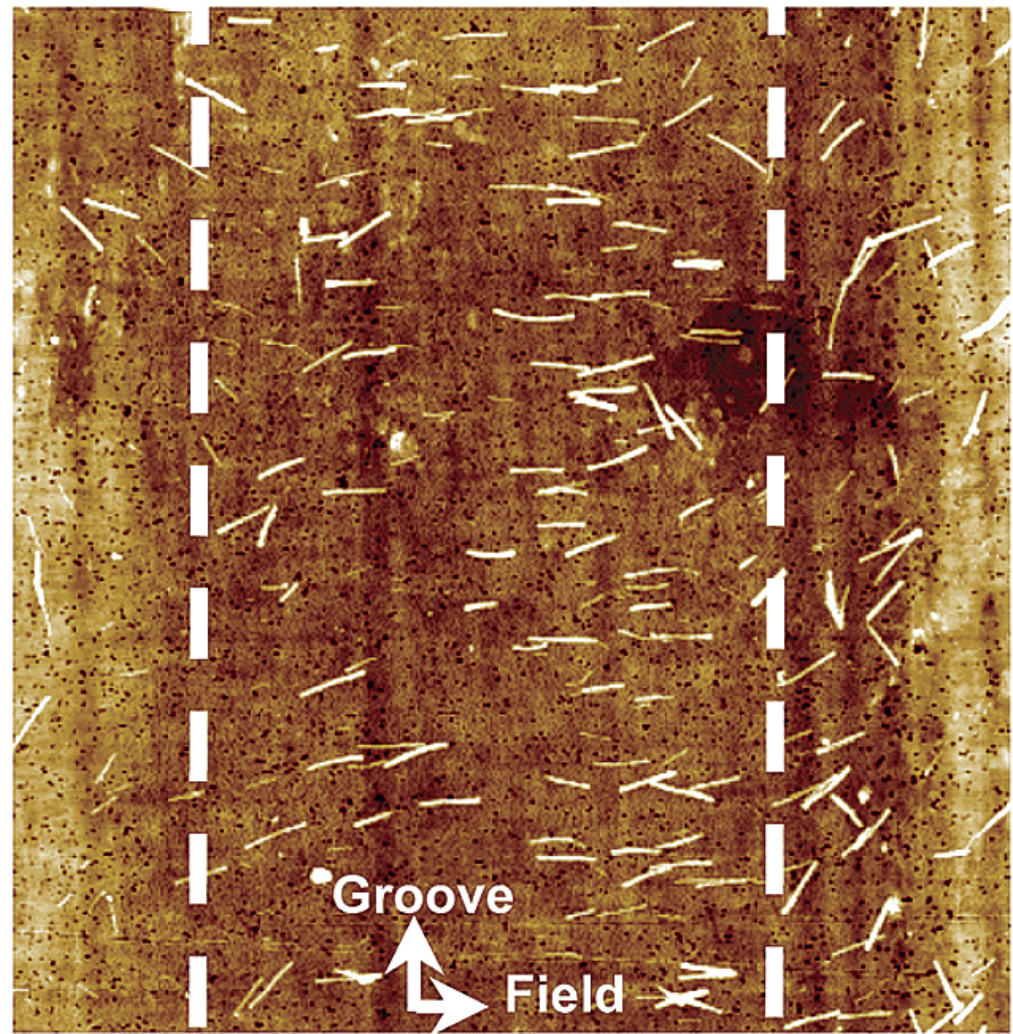
Nanotubes - Organisation

Oriented CNT films. CNTs deposited onto grooved polycarbonate membranes from LC solvents undergo spontaneous orientational ordering, as shown in these AFM images. In all cases the grooves were oriented vertically. Parts (a) and (b) show SWCNTs from E7 at low and high coverage. Dark spots are 100 or 200 nm diameter holes in the polycarbonate membrane through which the LC drains, leaving a thin film of CNTs. Both images measure $5 \times 5 \mu\text{m}$. (c) MWCNTs from 5CB ($50 \times 50 \mu\text{m}$).



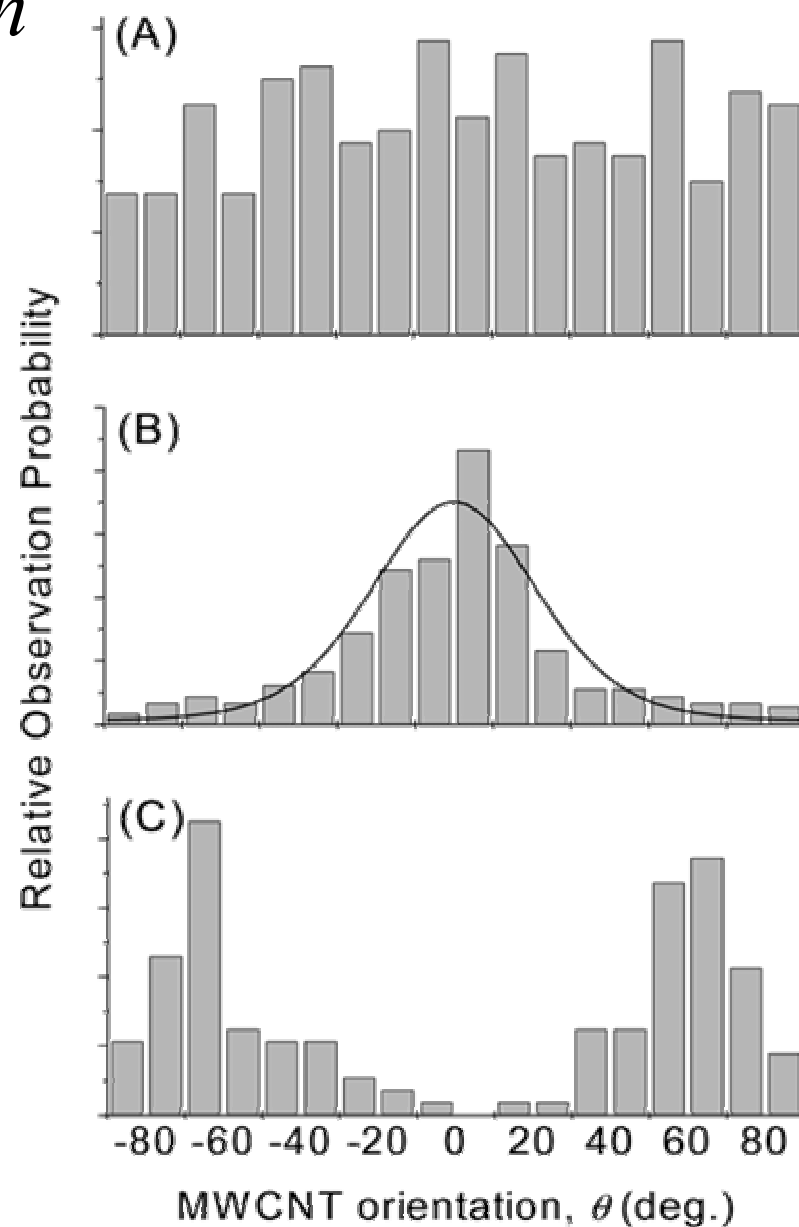
Nanotubes - Organisation

Electric field induced alignment. Microscopic patterning of CNT alignment can be achieved using local electric fields and LCs. This AFM image shows oriented MWCNTs deposited from 5CB in a 20 μm channel defined by two copper electrodes whose boundaries are indicated by dashed lines. A 1.8 V m^{-1} electric field was strong enough to overwhelm the orientational influence of the grooves, which were perpendicular to the electric field in the channel. Similar results were obtained for SWCNTs.



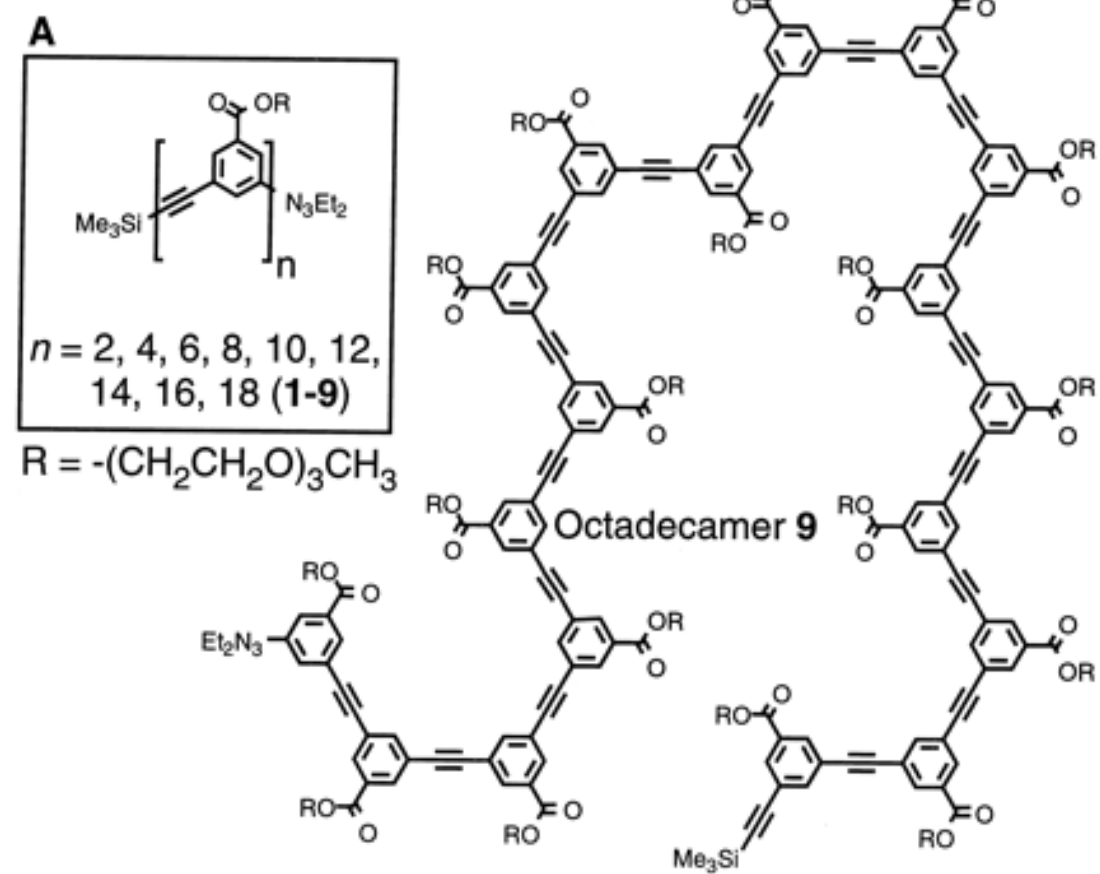
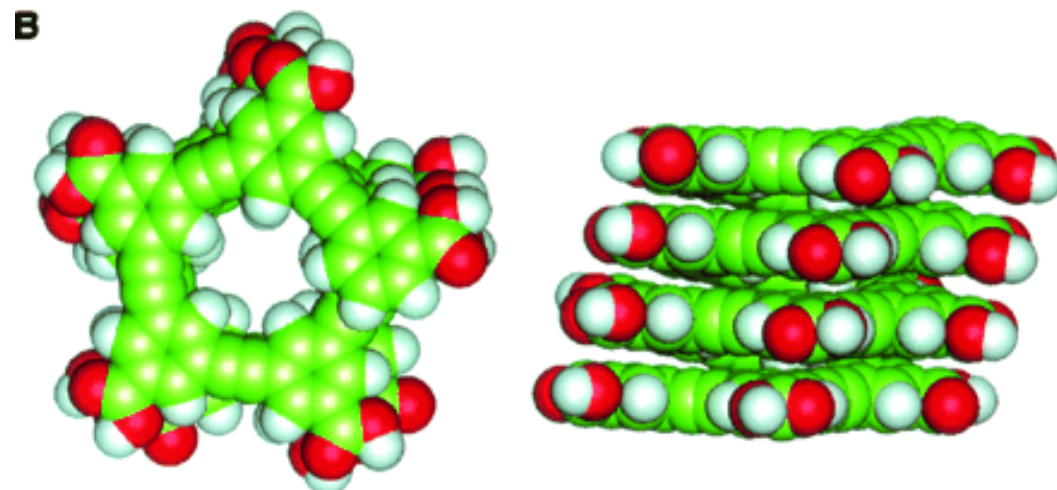
Nanotubes - Organisation

Quantification of long-range orientational order. The histograms show orientational distributions of MWCNTs in films prepared from suspensions of the LC 5CB by three different methods. The angle θ is the difference between the long axis of the CNTs and the average direction of substrate grooves. (a) Films prepared above the isotropic transition temperature of 5CB, where the LC behaves as a conventional liquid, show only random orientation (300 observations). (b) When deposited at room temperature, near the center of 5CB's nematic range, the LC director and CNTs align parallel to substrate grooves (361 observations). The solid line is a fit using the theory described in the text. (c) When deposition is performed in a magnetic field oriented in the substrate plane perpendicular to the grooves, the two alignment influences compete, leading to a bimodal distribution of alignment angles (160 observations).



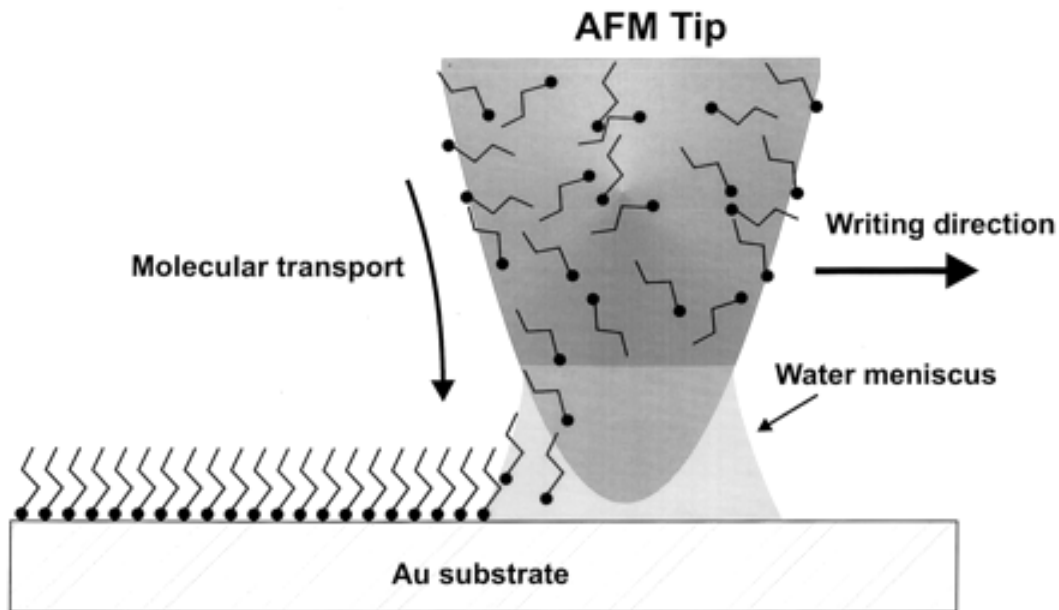
Self-Templating – 1-D

Oligo(phenylene ethynylene)**9** undergoes solvophobic driven folding into a helical conformation. The helix-coil equilibrium is illustrated with a space-filling model (side chains removed for clarity).

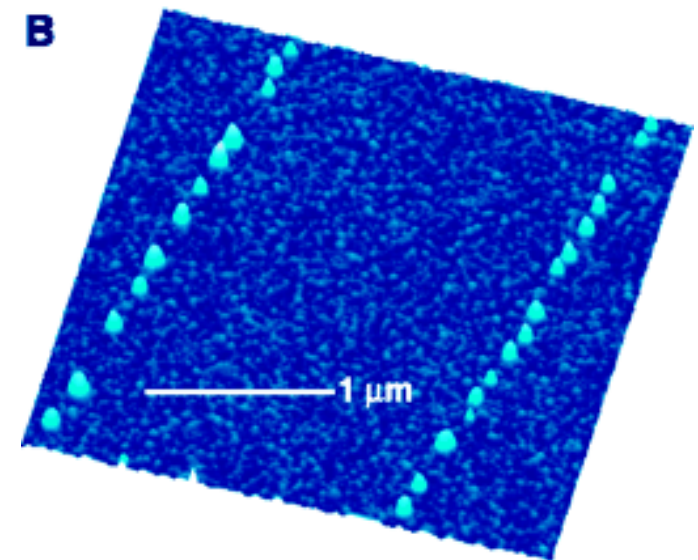
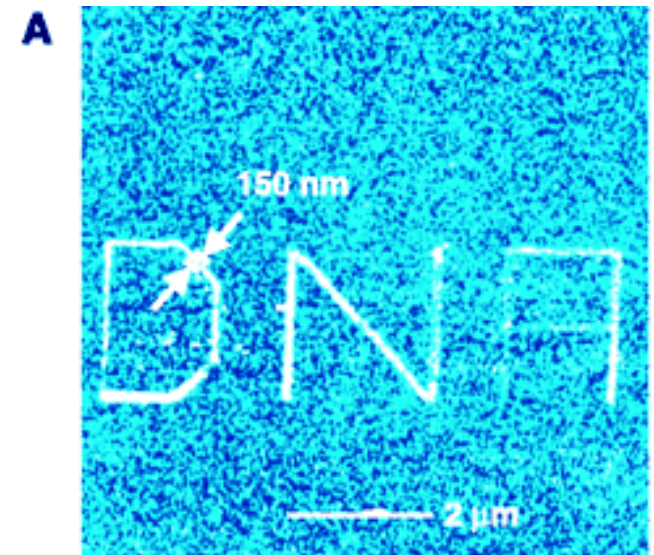


Templating – 1-D

Dip-Pen Nanolithography

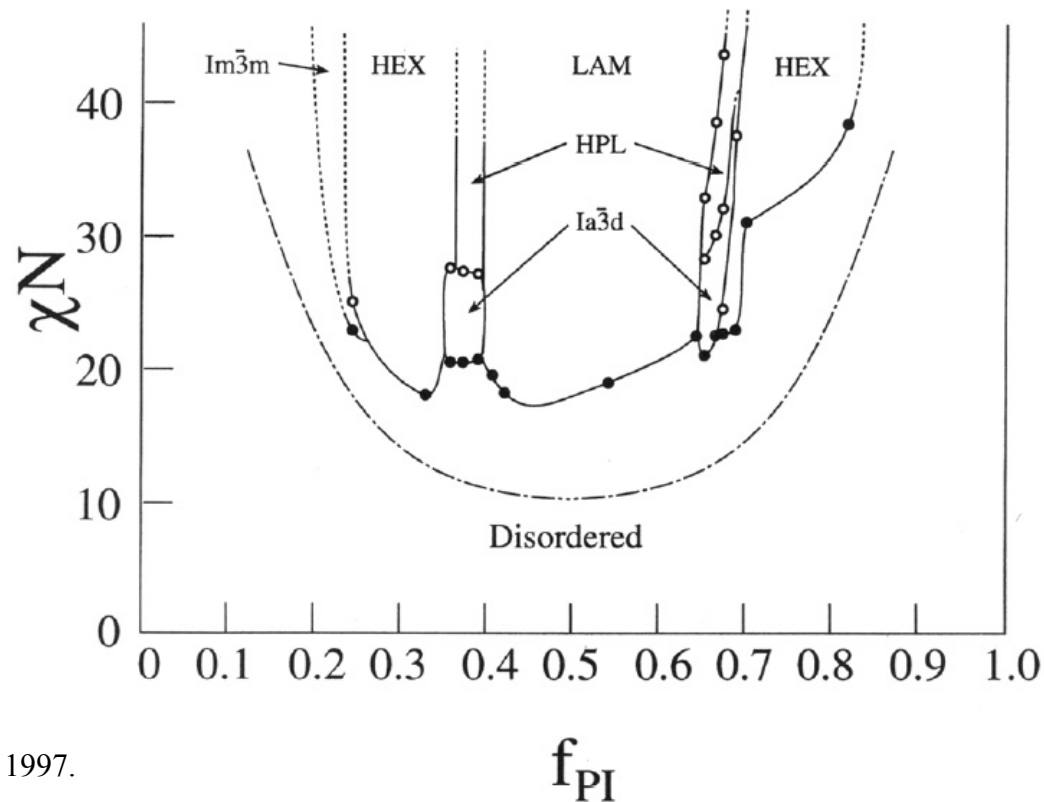
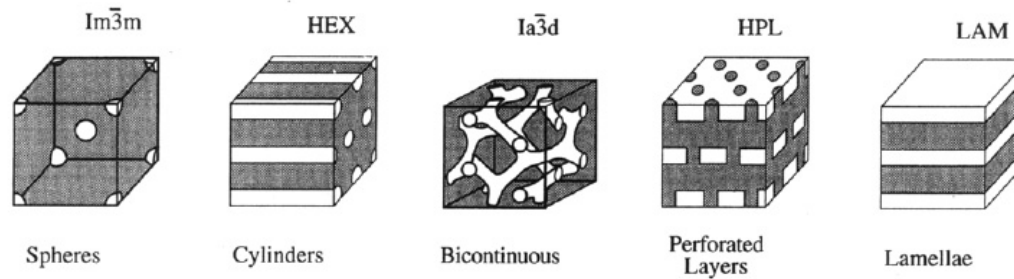


Schematic representation of DPN. A water meniscus forms between the AFM tip coated with ODT and the Au substrate. The size of the meniscus, which is controlled by relative humidity, affects the ODT transport rate, the effective tip-substrate contact area, and DPN resolution.

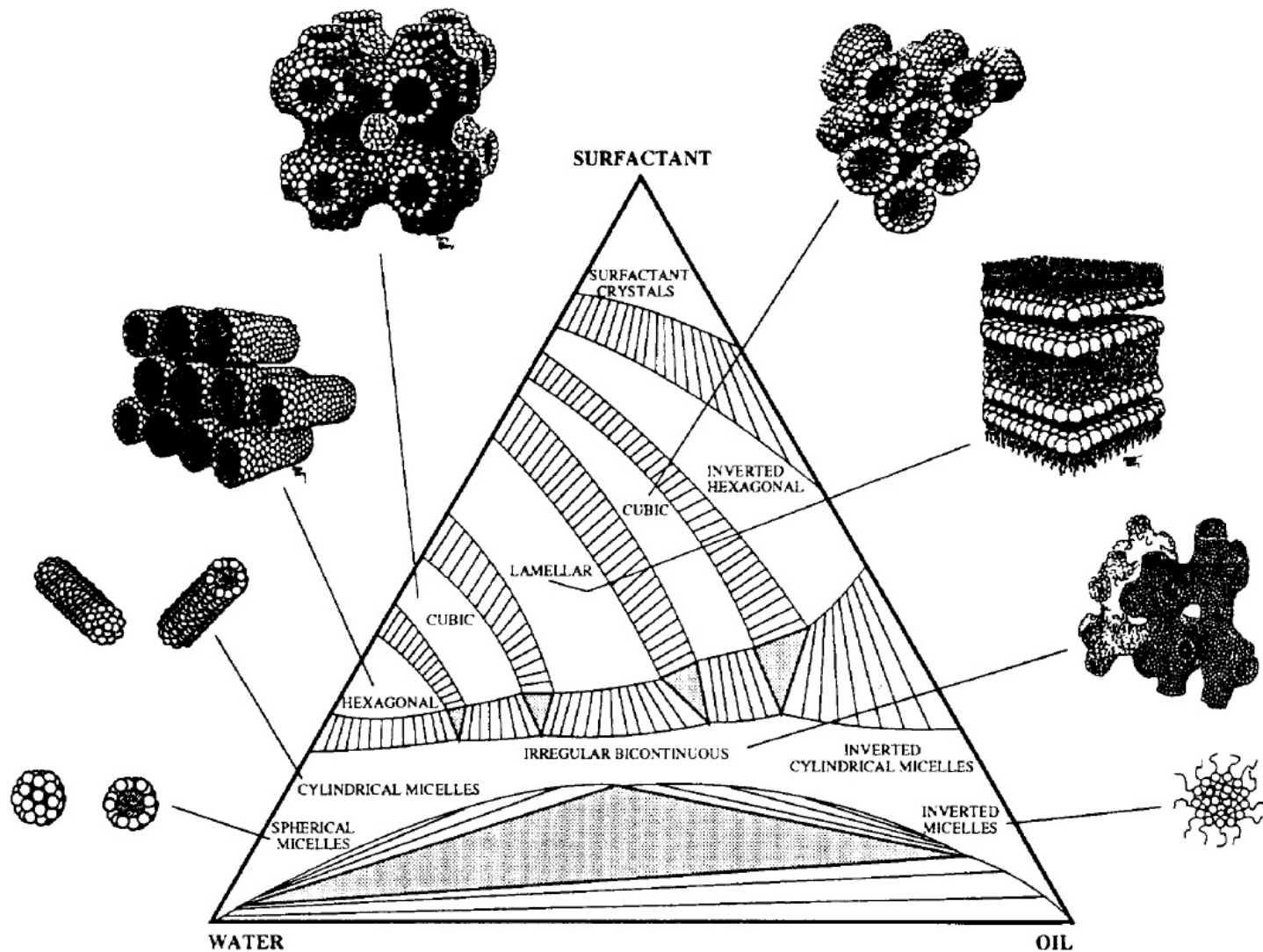


Templating – Block Copolymers

1-D, 2-D and 3-D

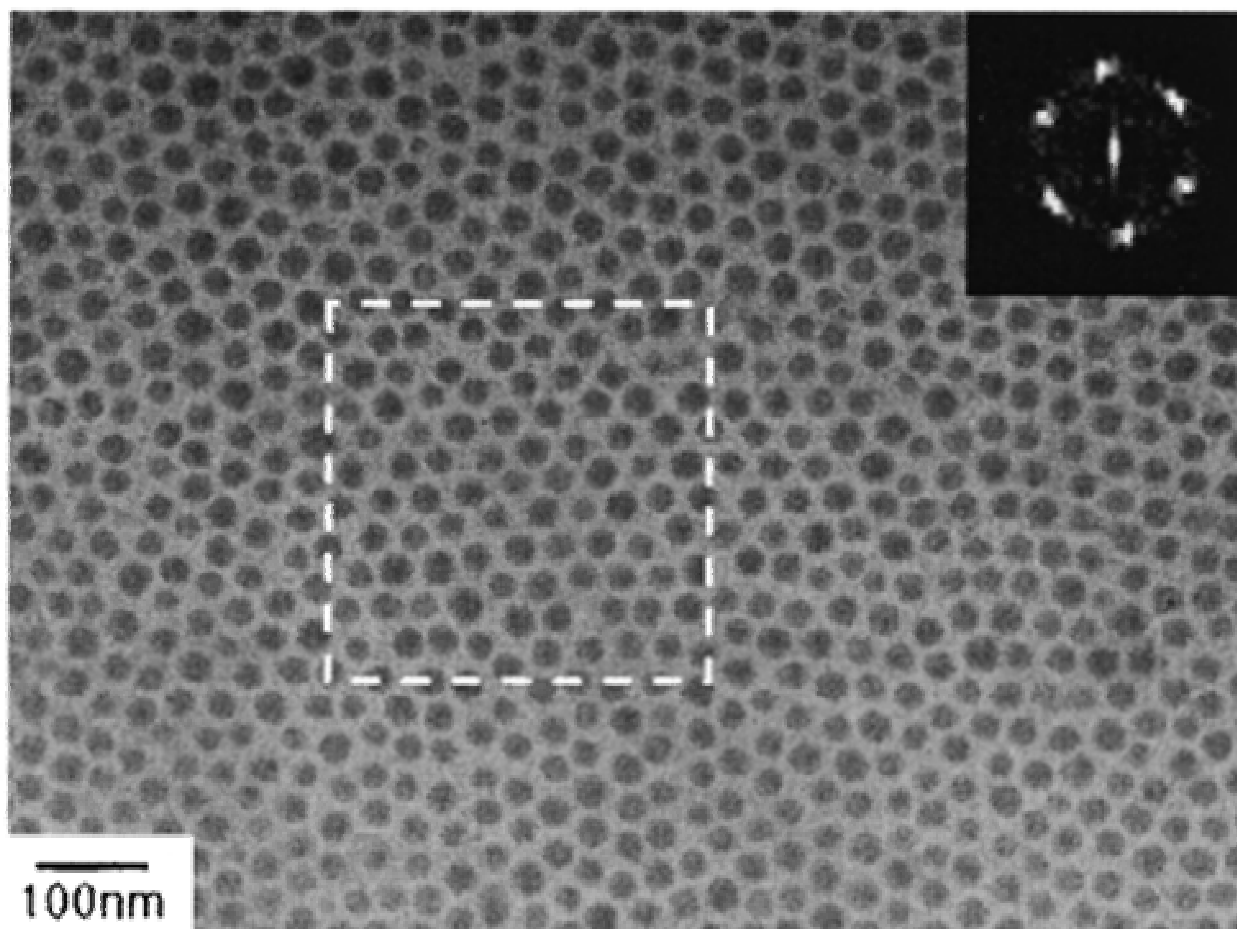


Templating - Ternary Surfactant Systems



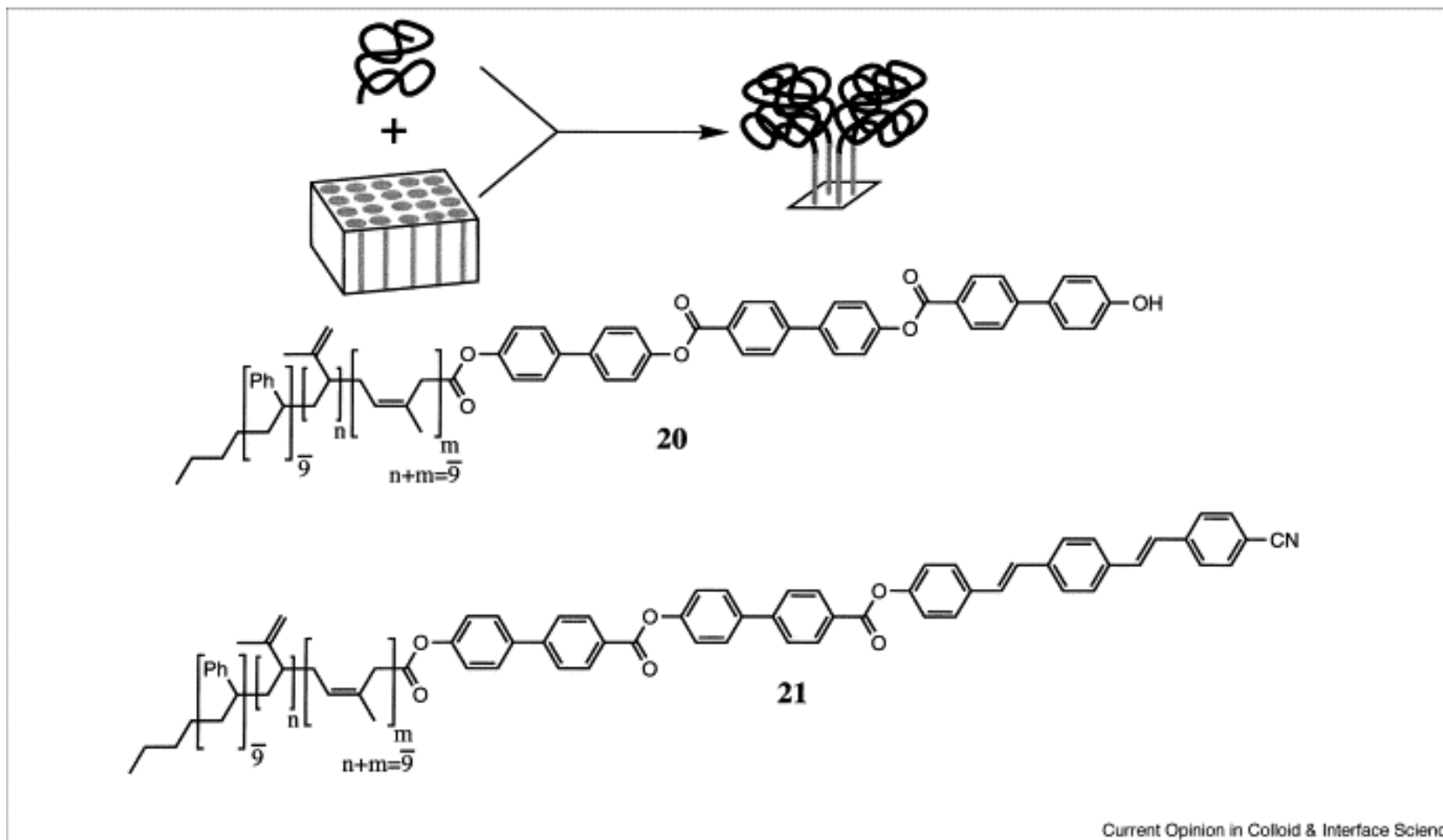
Nanopattern Diblock Copolymer Films

Plan-view TEM image of a free-standing monolayer film of PS-P4VP micelles. The P4VP block was selectively stained with I₂ and appeared as dark spherical cores. Inserted is a Fourier transformed pattern of the boxed area.



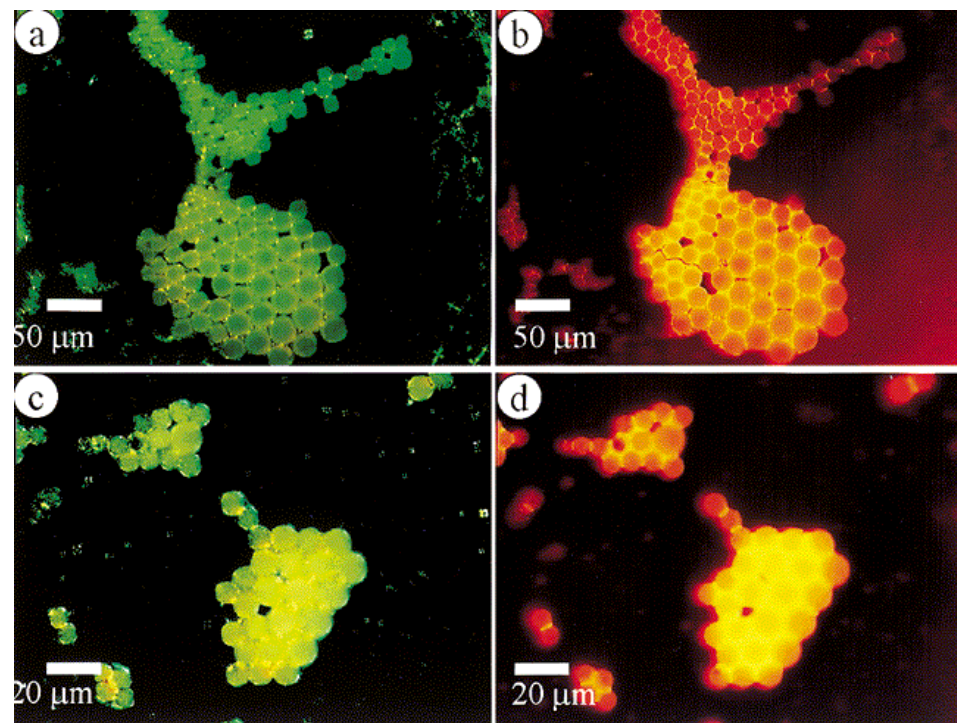
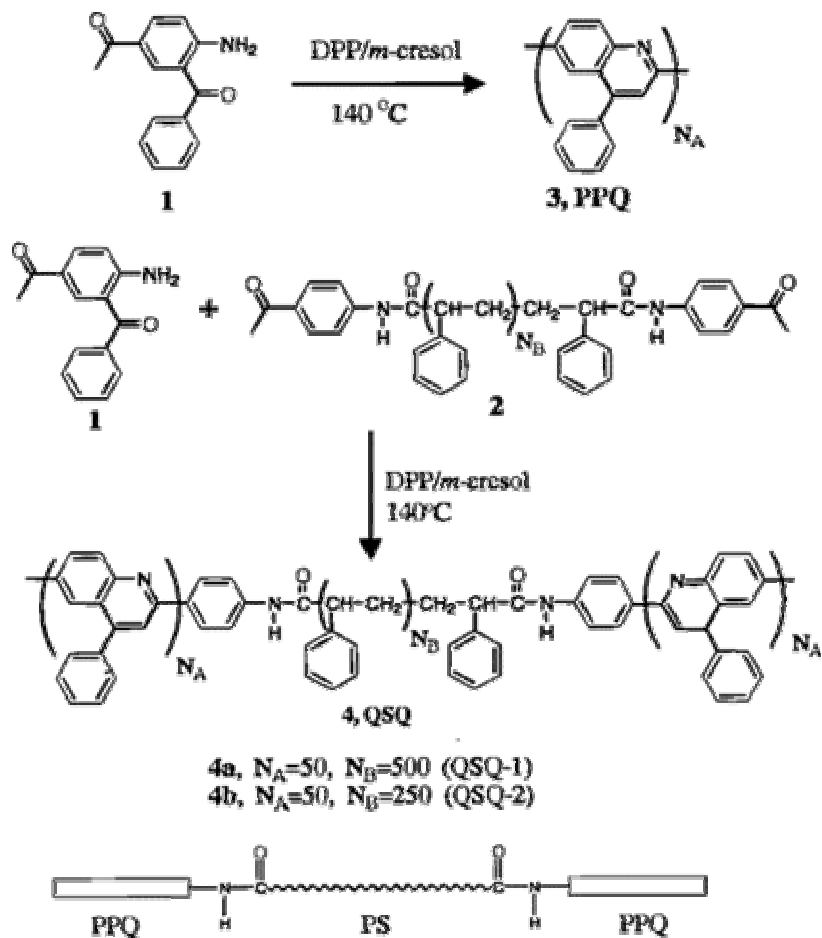
Self-Templating – 2-D

Figure 5



The schematic diagram illustrates the concept of producing finite supramolecular polymers by frustration of an infinitely periodic packing of rods. Rodcoil molecules **20** and **21** produce mushroom-shaped supramolecular polymers of nanoscale dimensions.

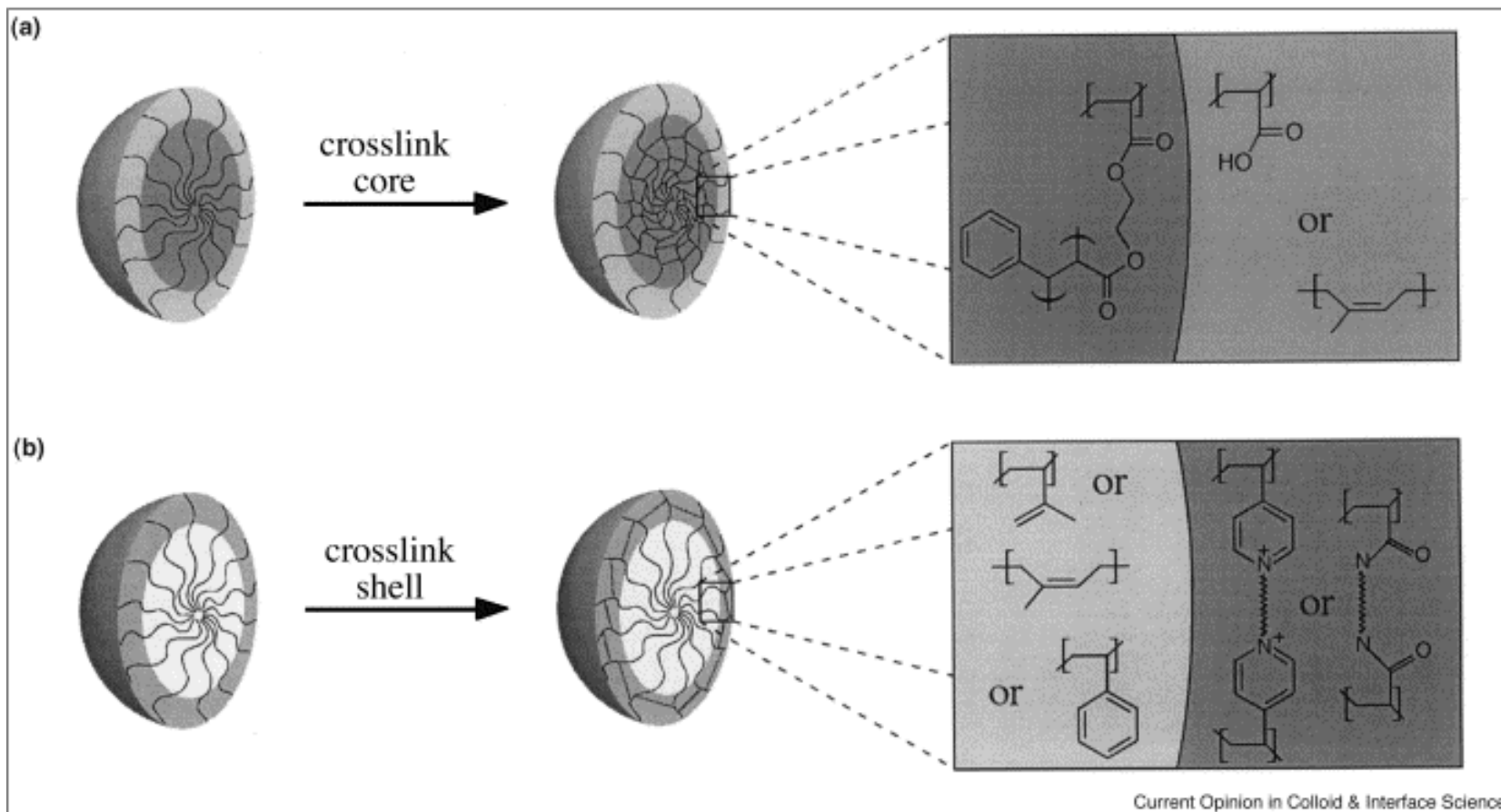
Templating – Triblock Copolymers



Polarized optical and fluorescence micrographs of solid microcapsules dried from QSQ-1 (a,b) and QSQ-2 (c,d) triblock copolymer dispersions. Images a and c were taken under cross-polarizers and the rest are fluorescence (540 nm excitation) images.

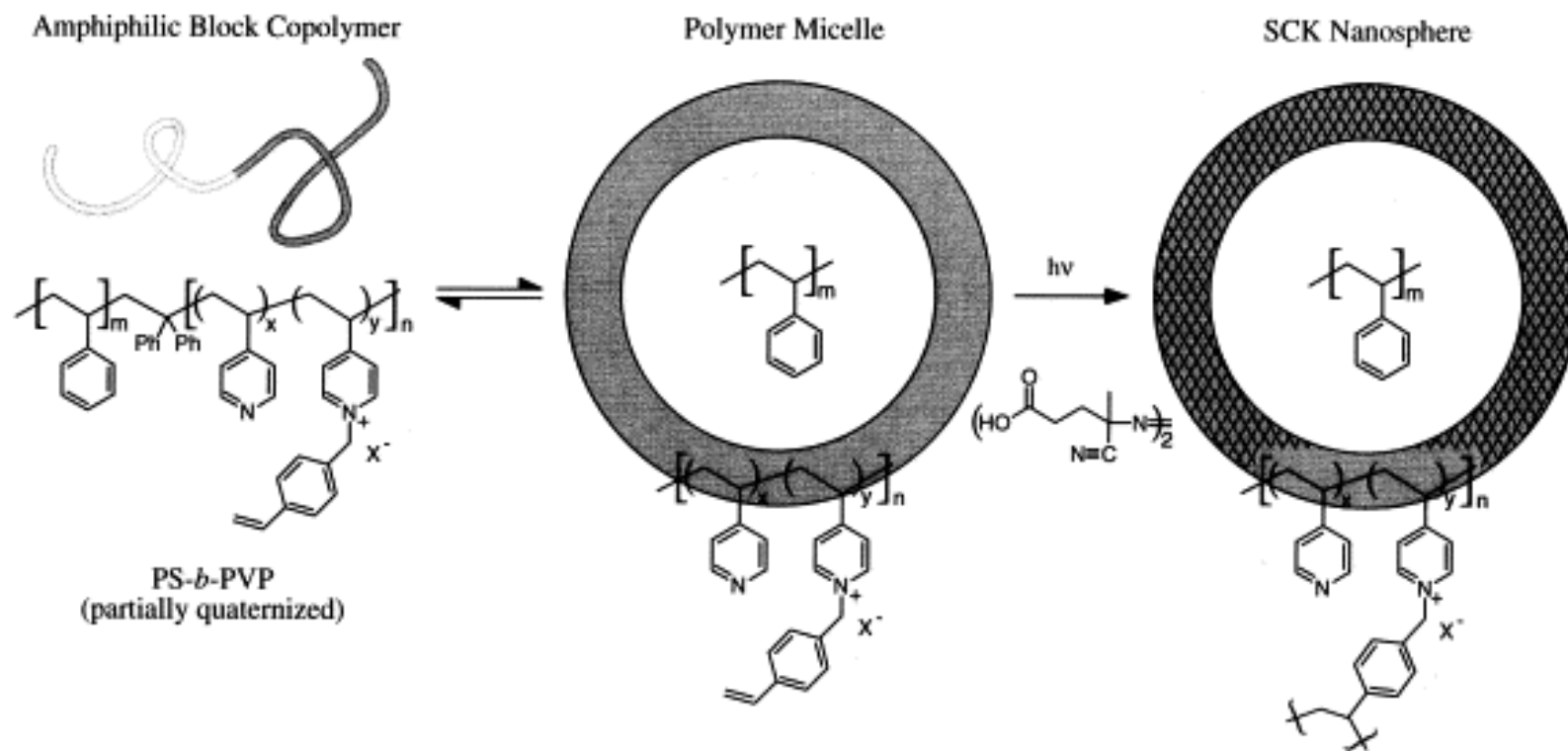
Templating – 3 D

Figure 3



Spherical polymer micelles in solution can undergo crosslinking reaction along the chains that compose the core or the shell to give (a) core-crosslinked nanospheres or (b) shell-crosslinked nanospheres, respectively. Assembly of the polymer micelles is driven by differing solubilities for the segments of diblock copolymers, whereas the stabilization of the structures is provided through covalent bond formation. The core-crosslinked structures have relied upon photopolymerization of cinnamoyl ethyl methacrylate groups to yield a network core domain and have contained hydrophobic or hydrophilic polymer chains attached to the core surface.

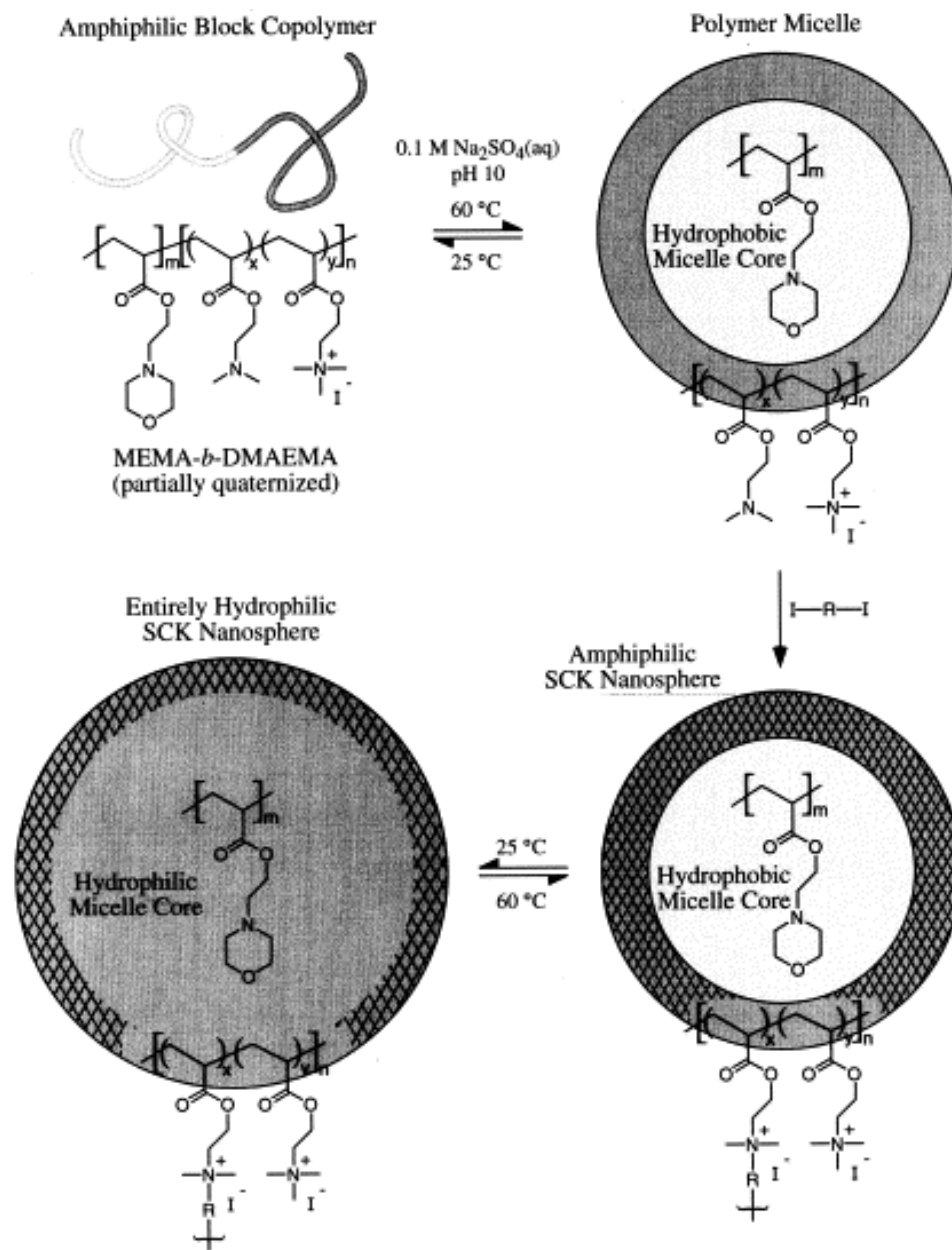
Templating – 3 D



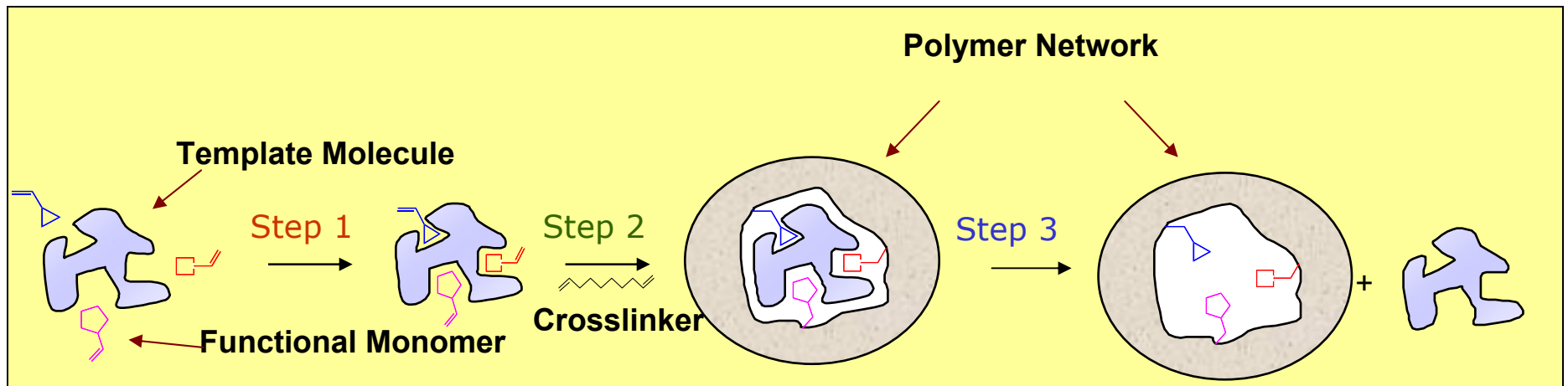
The first SCK nanosphere was prepared from a diblock copolymer of styrene and 4-vinylpyridine, of which a fraction of the vinylpyridine nitrogens were quaternized by reaction with *p*-chloromethylstyrene. The *p*-chloromethylstyrene introduced water-soluble salts and reactive styrenyl side chain functionalities. Solubilization in a mixture of tetrahydrofuran and water gave polymer micelles. Cross-linking throughout the shell was then accomplished by addition of a water-soluble radical initiator and irradiation. As the styrene chain length increased, relative to the vinylpyridine segment, the SCK nanosphere diameter increased.

Templating – 3 D

SCK nanospheres that exhibit reversible core hydrophilic/hydrophobic character were prepared by the incorporation of *N*-(morpholino)ethyl methacrylate (MEMA) as the core material. At 60°C, the MEMA is not water soluble, which allowed for micellization of block copolymers of MEMA and 2-(dimethylamino)ethyl methacrylate (DMAEMA), partially quaternized by methyl iodide. The shell was cross-linked via quaternization of remaining shell DMAEMA segments with 1,2-bis-(2-iodoethoxy)ethane, and then reversible hydration/dehydration by temperature variation was possible because of the stabilizing shell cross-links.

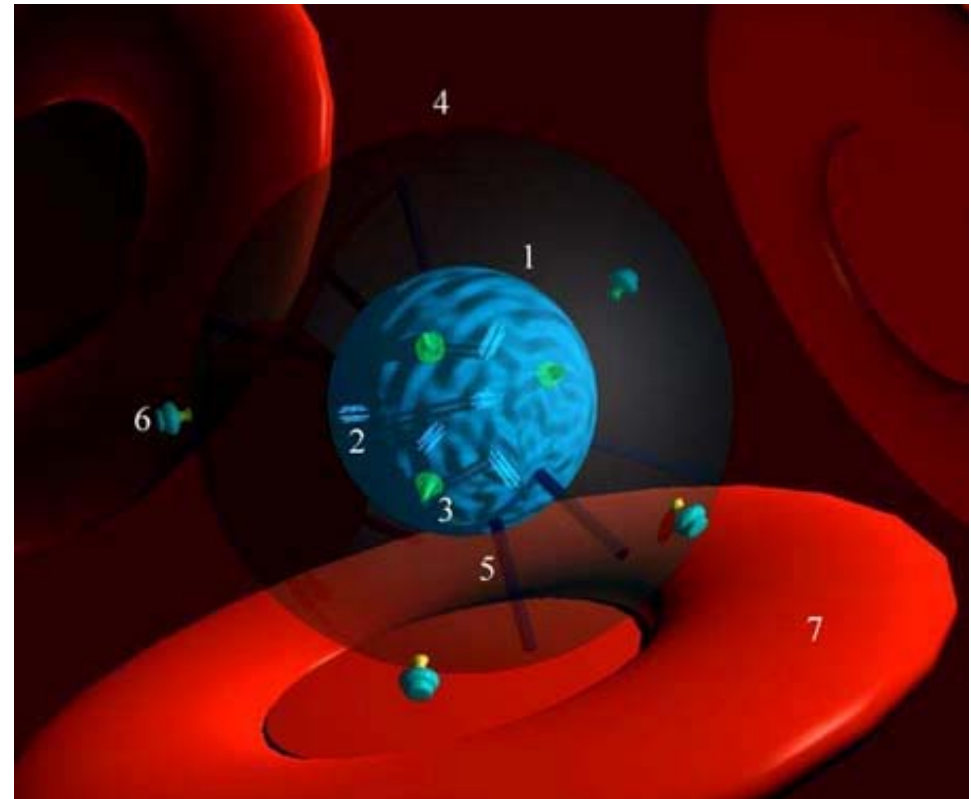


Templating 3D – Molecular Imprinting

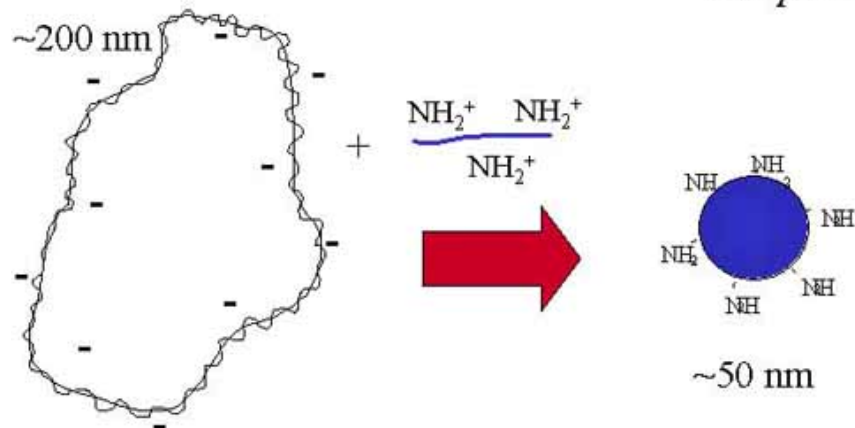


Gene Delivery

- 1=condensed DNA core
- 2=endosomal lytic peptide
- 3=nuclear targeting peptide
- 4=hydrophilic shield
- 5=cleavable linker
- 6=targeting element
- 7=erythrocyte



plasmid DNA + Polylysine (pLL) = pLL/DNA complex



The End...